DESIGN OF EXPERIMENTS APPROACH TO HELICOPTER ROTOR OPTIMIZATION

M.Senthil Murugan * **Ranjan Ganguli** †
Department of Aerospace Engineering, Indian Institute of Science,
Bangalore-560012, India.

Abstract

An optimization procedure to reduce oscillatory hub loads for a four bladed soft-inplane hingeless helicopter rotor is developed. The objective function to be minimized consists of scalar norms of 4/rev vibratory hub loads transmitted by a 4-bladed helicopter rotor to the fuselage. The mass and stiffness properties of the rotor blades are considered as the design variables. Constraints are imposed on the dynamic stresses caused by the blade root loads, and move limits on the design variables. An aeroelastic analysis based on finite elements in space and time is used to construct the response surface approximations for the objective function and constraints. The response surface approximations decouple the analysis problem from the optimization problem. The numerical sampling is done using the central composite design of the theory of design of experiments. The approximate optimization problem expressed in terms of quadratic response surfaces is solved using standard technique. Optimization results in forward flight with unsteady aerodynamic modeling show a reduction in the objective function of about 15 percent. The dominant loads in vehicle vibration are the vertical hub shear and the rolling and pitching moments which are reduced by 22-26 percent. The composite box-beam corresponding to the section properties predicted by the aeroelastic optimization is designed using genetic algorithm.

Nomenclature

a	lift curve slope
c	blade chord
$\mathbf{C}$	blade damping matrix
EI_y	flap bending stifness
EI_z	lag bending stifness
$f(\mathbf{X})$	objective function
$\mathbf{F}$	blade load vector
$F_x^{np}, F_y^{np}, F_z^{np}$	n/rev rotor hub shear forces
$g_j(\mathbf{X}), h_k(\mathbf{X})$	constraints
GJ	torsional stifness
I_b	blade mass moment of inertia
J_v	objective function
J_{dn}^i	scalar norm of n/rev blade root bending moments
$\mathbf{K}$	blade stiffness matrix at the i^{th} iteration
m	blade section mass
m_0	reference blade section mass
$\mathbf{M}$	blade mass matrix
$M_x^{np}, M_y^{np}, M_z^{np}$	n/rev rotor hub moments
$\mathbf{p}$	modal displacement vector
R	blade radius
u_j, v_k	penalty parameters
$\beta_0, \beta_i, \beta_{ij}$	coefficients of the response surface model
Ω	rotor rotational speed
γ	lock number
ρ	density of the air

Introduction

In a helicopter, the main rotor is the crucial subsystem, which provides lift, propulsive force and control capability of the helicopter. Therefore, the design of main rotor is an important problem that has received considerable attention. The design of the helicopter rotor involves a variety of aerospace engineering disciplines. Rotor blades are slender flexible beams, which can undergo elastic deformations in bending and torsion, that can be beyond the limits of linear beam theories. The deflections of the blade interact with the aerodynamic loading. The rotor blade aerodynamics in turn, is coupled with the structural dynamics because much of the elastic deformation and damping in flap and lag bending and in torsion is of aerodynamic

*Research Scholar,
†Assistant Professor.

origin. Therefore, the prediction of helicopter blade and hub loads is an integrated aeroelastic problem. Helicopter rotor aeroelastic analysis have been developed by academic institutions and helicopter companies are widely used for preliminary design of the helicopter rotor blades.

One of the chief issues in the helicopter industry is the minimization of vibrations on the helicopter airframe, which are caused by an unsteady aerodynamic environment and highly flexible rotating blades. The vibratory bending moments acting along the blade length also causes dynamic stresses, at several harmonics of the rotational speed, on the rotor blade. These dynamic stresses cause structural fatigue, leading to a reduction in blade life. The critical dynamic stresses generally occur at the spanwise location where the vibratory bending moment is highest. For the hingeless rotors, it occurs at the blade root. Therefore, a direct approach for increasing the life of the blade is to design the rotor to produce low vibratory bending moments. The changes of mass and stiffness along the blade chord and span direction affect the structural dynamics and aeroelastic behavior as well as the stress distribution.

In recent years, considerable research has been directed towards the application of aeroelastic optimization methodology for the vibration reduction problem. Ganguli and Chopra [1] carried out aeroelastic optimization studies out for rotor blades with swept tips and for composite rotors. Yaun and Friedmann [2] carried out a structural optimization study for vibration reduction of a composite rotor blade with a swept tip. Chattopadhyay *et al* [3, 4] have done extensive work on the optimization of helicopter rotors and prop rotors. Other recent studies in helicopter rotor optimization includes those by Kim and Sarigul-Klijn [6] for articulated rotors, Soykasap and Hodges [7] for composite tilt rotors, and Celi *et al* [8]-[9] addressing maneuver flight. A recent review on helicopter optimization is provided by Celi [10]. In the above aeroelastic optimization studies, quasi-steady aerodynamic model is used in the rotor aeroelastic analysis.

The helicopter rotor dynamics analysis involves complex computer analyses, which are computationally expensive to perform. These analyses involve the solution of nonlinear rotor dynamics equation, obtaining the helicopter trim condition and aeroelastic stability condition. In the conventional aeroelastic optimization studies, the large aeroelastic analysis program has to be integrated with the optimization software, which can make the problem a cumbersome task. Gradient based approaches to optimization require that the sensitivity derivatives either be calculated analytically or by finite difference. Finite difference derivatives are computationally expensive to calculate and the selection of an appropriate step size can be difficult. Analytical and semi analytical derivatives have been used by Spence and Celi [9], Murthy and Lu [11], Lim and Chopra [12], and Ganguli and Chopra [1, 17]. These derivatives are obtained using chain rule differentiation and included in the computer program for aeroelastic analysis as an integral part. Analytical derivatives are more accurate than finite differences and large savings of computer time are possible. However certain approximations such as ignoring the changes in trim conditions and blade normal modes due to changes in design variables are often made in calculation of analytical derivatives. These assumptions appear to have been reasonable for the vibration reduction problems. A key problem of analytical derivatives is linked to the issue of the software aging. With the passage of time, changes are made in the aeroelastic analysis to account for refinements in physical modeling. When such changes are made, the analytical derivatives must also be updated. This is not always possible as the domain experts performing physical modeling may not be aware of the optimization aspects of the software. Furthermore, in the industry setting the rotor aeroelastic analysis codes are considered as proprietary and it is very difficult to make changes inside them. Therefore analytical derivatives are difficult to implement in an industry setting.

One approach to overcome this difficulty is to use statistical techniques to construct approximations of the analyses that are much more efficient to run and easier to integrate together, and yield insight into the functional relationship between the objective function and design variables [13]. This results in the construction of the approximations of the analyses, instead of integrating the computer programs. Response surface (RS) methodology is one such statistical method used to construct approximations [14]. Response surfaces for objective and constraint functions are created by sampled numerical experiments over the design space [15]. The response surface models created then replaces the computationally expensive analyses and facilitates fast analysis and exploration of the design space. Low order polynomials are mostly used as the response surface approximating functions.

In helicopter aeroelastic optimization very limited work has been done using response surfaces. Henderson, Walsh and Young [16] have applied response

surface techniques to helicopter rotor blade optimization. They used multilevel decomposition approach in optimization. A large complex optimization problem was broken into a hierarchy of smaller optimization subproblems. The upper level objective function was a linear combination of performance and dynamic measures. Upper level design variables include pretwist, blade stifnesses, tuning masses and tuning locations. The lower level optimization assures that a structure can be sized to provide the stiffnesses required by the upper level and assures the structural integrity of the blade. The analysis proceeds from the upper level to lower level while the optimization proceeds from the lower level to the upper level. However, in the study [16] response surface approximations are used for the cross-section design problem and not as an approximation to the rotor aeroelastic analysis.

The rotor blade cross-section design problem links blade cross sectional properties with one dimensional beam properties that are typically used for aeroelastic analysis. Typically, the load carrying member in a rotor blade consists of a box-beam blade spar. Hajela *et al.* [5] used neural surrogate functions in the optimization. The objective function and constraints were approximated by the neural surrogate functions. The neural networks, though are good universal function approximations, have a black-box nature and are difficult to use in an industry setting. In contrast, polynomial response surfaces are easy to understand and capture the key slopes and curvatures of the design space while smoothing out local changes which avoids the problem of spurious local minima.

The objective of this study is to perform an aeroelastic optimization of a helicopter rotor, using response surface approximations to the rotor aeroelastic analysis in the upper level problem. The helicopter aeroelastic analysis is based on a finite element method in space and time. To reduce helicopter vibrations, the objective function includes all six components of 4P hub loads for a four bladed hingeless rotors, while maintaining the constraints on dynamic stresses developed on the rotor blade, which are caused primarily by the 1/rev and 2/rev rotating frame loads. This paper approaches the problem of vibration reduction by developing an RS model for the objective function, instead of doing the rotor dynamic analyses for each function evaluation required by the optimization process. The response surface approximated optimization problem is then solved using standard gradient based algorithms.

The lower level problem of composite box-beam design is solved using genetic algorithm. The ability of genetic algorithm to handle discrete design variables is used for obtaining the composite ply layups with $[0^o, (\pm 45^o), (\pm 90^o)]$ ply angles. Another feature of this study is the use of sophisticated unsteady aerodynamic model including impulsive and attached flow aerodynamics which causes numerous convergence problems in aeroelastic analysis. Note that the quasi-steady aerodynamic model was used in the previous optimization studies and convergence problems were not encountered [1, 17]. The response surface approximations for the rotor aeroelastic analysis are used to overcome the numerical convergence problems caused by the unsteady aerodynamic model.

Helicopter Rotor Dynamic Analysis

In this work, a comprehensive aeroelastic analysis code, based on finite element method is used to evaluate the resultant forces of the rotor. The rotorcraft structure is modeled as a nonlinear representation of elastic rotor blades coupled to a rigid fuselage. The blade is modeled as a slender elastic beam undergoing flap bending, lag bending, elastic twist, and axial deflection. The effect of moderate deflections is included by retaining second order non-linear terms [18]. The blade is discretized into beam finite elements, each with fifteen degrees of freedom. The finite element equations are reduced in size by using normal mode transformation. This results in the non-linear ordinary differential equation with periodic coefficients as given below.

$$\mathbf{M}\ddot{\mathbf{p}} + \mathbf{C}\dot{\mathbf{p}} + \mathbf{K}\mathbf{p} = \mathbf{F}(\mathbf{p}, \dot{\mathbf{p}}) \qquad (1)$$

Here **M**,**C**,**K** and **F** represents the finite element mass matrix, structural stiffness matrix, damping matrix and finite element force vector, respectively. These equations are then solved using finite element in time in combination with the Newton-Raphson method. The finite element in time approximation is especially suited for periodic systems [19]. The above equations govern the dynamics of the rotor blade. The solutions to the equations are then used to calculate rotor blade loads using the force summation method, where aerodynamic forces are added to the inertial forces. The blade loads are integrated over the blade length and transformed to the fixed frame to get hub loads. The steady hub loads are used to obtain the forces acting on the rotor and combined with fuselage and tail rotor forces to obtain the helicopter rotor trim equations.

$$\mathbf{F}(\theta) = \mathbf{0} \qquad (2)$$

These nonlinear trim equations are also solved using the Newton-Raphson method. The helicopter rotor trim equations and the blade response equations in (1) and (2) are solved simultaneously to obtain the blade steady response and hub loads. This coupled trim procedure is important for capturing the aeroelastic interaction between the aerodynamic forces and the blade deformations. Further details of the analysis are available from the reference [20].

Response Surface Modeling

Response surface modeling techniques have been used in the past few years to solve complex, computationally intensive engineering problems [21]. Design of Experiments(DOE) theory provides a systematic means of selecting the set of points in the k dimensional design space, at which to perform computational analyses. By using the RS techniques, the analysis codes are separated from the optimization codes. The complex analysis codes are replaced by the simple polynomials. Second order or quadratic polynomials are mostly used.
A quadratic RS model in k variables of the form,

$$y = \beta_0 + \sum_{i=1}^{k} \beta_i x_i + \sum_{i=1}^{k} \sum_{j=1}^{i} \beta_{ij} x_i x_j \qquad (3)$$

is used in this paper. The second order model described in the above equation is a widely used model to describe experimental data in which system curvature is present. The above equation contains $1 + 2k + k(k-1)/2$ parameters. As a result, the experimental design used must contain at least $1 + 2k + k(k-1)/2$ distinct design points. In addition, the design must involve at least three levels of each design variable to estimate the pure quadratic terms. There are families of designs available, for fitting the second order model. The central composite designs(CCDs) is one of the popular class of second-order designs. It involves the use of a two level factorial or fraction combined with the $2k$ axial or star points. As a result, the design involves, 2^k factorial points, $2k$ axial points, and n_c center runs. The factorial points represent a variance optimal design for a first order model or a first-order+two-factor interaction type model. Center runs provide information about the existence of curvature in the system. If curvature is found in the system, the addition of axial points allow for efficient estimation of the pure quadratic terms. The choice of α, the axial distance, depends to a great extent on the region of operabilty and region of interest. The values of axial distance varies from 1.0 to $\sqrt{k}$. For the $k = 2$ case the value of α, the axial distance is $\sqrt{2}$. Figure (1) shows the

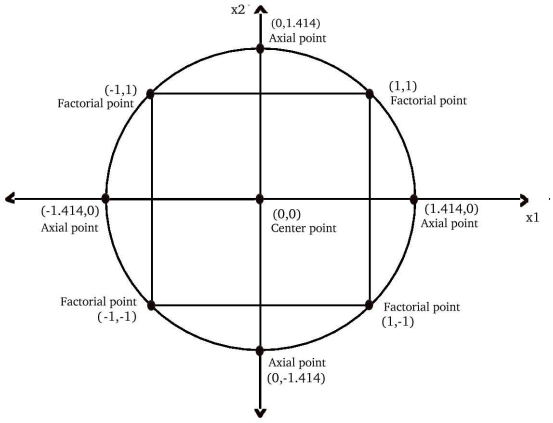

Figure 1: Central Composite Design for $k = 2$

CCD for $k = 2$. In this case, for $k = 2$, there are $4(2^k)$ factorial points, 4 $(2 * k)$ axial points and one center point resulting in 9 points. Also note that for $k = 2$, there are $1 + 2k + k(k-1)/2 = 6$ regression coefficients need to be determined to find the second order response surface as shown in equation(20). The CCD design therefore overfits the points to obtain the response surface. It is therefore able to reduce the error present in any one of the points and avoid the local minima that are not robust and have high sensitivity to change in the design variables.

In this work, the constraints were appended to the objective function $f(\mathbf{x})$, using a quadratic exterior penalty function, which is of the form

$$P(\mathbf{X}) = f(\mathbf{X}) + \sum_{j=1}^{J} u_j max[0, g_j(\mathbf{X})]^2 + \sum_{k=1}^{K} v_k (h_k(\mathbf{X}))^2 \qquad (4)$$

where, $g_j(\mathbf{X}), h_k(\mathbf{X})$ are the equality and inequality constraints, respectively expressed in the form, $g_j(\mathbf{X}) \leq 0$ and $h_k(\mathbf{X}) = 0$. The u_j and v_k represents the penalty parameters.

Problem Description

The objective function J_v used in this study represents the vibratory hub loads and has been used as a measure of rotorcraft vibration [1, 2]. The objective

function is the sum of the scalar norms of the N/rev forces and the N/rev moment's transmitted by an N-bladed helicopter rotor to the fuselage as the primary source of vibration. In this work, 4/rev hub force resultant and, 4/rev hub moment resultant of a four bladed rotor is used as the objective function J_v. The objective function is of the form

$$f(\mathbf{X}) = J_v = \sqrt{(F_x^{4p})^2 + (F_y^{4p})^2 + (F_z^{4p})^2} + \sqrt{(M_x^{4p})^2 + (M_y^{4p})^2 + (M_z^{4p})^2} \quad (5)$$

where the forces and moments are non-dimensionalized with respect to $m_0\Omega^2R^2$ and $m_0\Omega^2R^3$, respectively. In the above equation F_x, F_y and F_z represents the longitudinal, lateral and vertical dynamic forces acting on the hub and, M_x, M_y and M_z are the rolling, pitching and yawing moments acting on the hub, respectively.

In the helicopter rotor, the loads observed in the rotating frame are periodic and can be expressed in terms of Fourier series. The first harmonic of these loads in the rotating frame is generally dominant and the magnitude of the harmonics declines with the higher harmonics. The 4/rev hub loads in the fixed frame come from the 3/rev, 4/rev and 5/rev in the rotating frame. Attempts to minimize the 4/rev hub loads for a four bladed hingeless rotor in forward flight can result in an increase in the 1/rev and 2/rev blade loads, causing higher dynamic stresses. The lower harmonic blade loads which are higher in magnitude are the main sources of dynamic stresses. Therefore, the constraints are imposed on the dynamic stresses caused by the 1/rev and 2/rev blade root bending moments. These constraints avoid reducing the fatigue life of the blade. The constraints are given by

$$J_{d1}^i \leq J_{d1}^o \quad (6)$$

$$J_{d2}^i \leq J_{d2}^o \quad (7)$$

where J_{d1}^i, J_{d2}^i are the scalar norm of 1/rev and 2/rev blade root bending moments at the i^{th} iteration of optimization, which are given below,

$${J_{d1}}^i = [\sqrt{(M_x^{1p})^2 + (M_y^{1p})^2 + (M_z^{1p})^2}]^i \quad (8)$$

$${J_{d2}}^i = [\sqrt{(M_x^{2p})^2 + (M_y^{2p})^2 + (M_z^{2p})^2}]^i \quad (9)$$

Here J_{d1}^0, J_{d2}^0 are the baseline values of the same 1/rev and 2/rev dynamic stresses respectively. To ensure the design variables stay within the region where the response surface is valid, a constraint is added. For the two design variables, it is found that constraining the design variables with in the circle as shown in the figure(1) is effective. And the constraint is given by,

$${x_1}^2 + {x_2}^2 \leq 2 \quad (10)$$

where the $x_1$and x_2 are coded variables used in the design of experiments and can be converted to physical variables using a linear transformation. For example, the levels $+1$ and -1 of the coded variable x_1 in the figure (1) can correspond to 5 percent increase and decrease from the baseline value of the blade mass, respectively. The baseline value of the mass corresponds to the center point in the x_1 direction. Similarly for the coded variable x_2, the $+1$ and -1 can correspond to 25 percent increase and decrease from the baseline value of the torsional stiffness. Therefore, once the baseline design at the center point is selected, the factorial points can be defined as percent changes in the baseline and the axial points are calculated using a linear transformation.

Numerical studies showed that the constraint in equation (10) was necessary to prevent the design from going in regions where the response surface approximation is not valid. Though the response surface approximation showed a reduction in vibration in a region beyond the constraint given in equation(10), the rotor analysis values showed an increase in the vibration with the same design variables values. It was also found that a square region [i.e, $-\sqrt{2} \leq x_1 \leq \sqrt{2}$, $-\sqrt{2} \leq x_2 \leq \sqrt{2}$] rather than the circular region also led to this problem. Thus the circle shown in figure(1) acts as a good bound inside which the response surfaces developed for this problem are valid. Expanding the formulation (10) to k design variables, the constraint can be expressed in the form,

$${x_1}^2 + {x_2}^2 + {x_3}^2 + ... + {x_k}^2 \leq k \quad (11)$$

The design variables are constrained to remain with in the hypersphere of radius $\sqrt{k}$. The three constraints used in this work can be written in standard notation as,

$$\begin{aligned} g_1(\mathbf{X}) &= {J_{d1}}^i - {J_{d1}}^0 \\ g_2(\mathbf{X}) &= {J_{d2}}^i - {J_{d2}}^0 \\ g_3(\mathbf{X}) &= \sum_{i=1}^{k} {x_i}^2 - k \end{aligned} \quad (12)$$

The composite objective function can then be written as,

$$P(\mathbf{X}) = f(\mathbf{X}) + u_1[max(0, g_1(\mathbf{X}))]^2 + u_2[max(0, g_2(\mathbf{X}))]^2 + u_3[max(0, g_3(\mathbf{X}))]^2 \quad (13)$$

where are u_1, u_2 and u_3 are the penalty parameters.

Results and Discussion

For the numerical study, a four bladed soft-inplane hingeless rotor blade which is uniform blade equivalent of the BO105 rotor blade is considered. The rotor properties used in this study are shown in the Table(I).

Table I: Baseline Hingeless Blade Properties

Number of blades	4
Radius (m)	4.94
Hover tip speed, m/s	198.12
m_o (kg/m)	6.46
$EI_y/m_o\Omega^2R^4$	0.0108
$EI_z/m_o\Omega^2R^4$	0.0268
$GJ/m_o\Omega^2R^4$	0.00615
m/m_o	1.0
Lock number	5.2
solidity	0.07
C_T/σ	0.07
c/R	0.055

An advance ratio of 0.3, which simulates forward flight condition is used to obtain the numerical result.

Two Design Variables

To have the geometric representation of the RS model and a better understanding of the method, only two design variables are considered initially. These variables are selected as the blade mass and the torsional stiffness, and are selected as they have been observed to have a strong influence on rotor vibration from earlier studies [1]. The Lock number has to be updated with the change in the values of the mass. The Lock number(γ) is defined as $\gamma = \rho acR^4/I_b$. Here ρ is density of the air, a is the lift curve slope, c is the blade chord, R is the rotor radius and I_b is the mass moment of inertia of the rotor blade. Thus, as the blade mass changes I_b changes resulting in a change in the Lock number.

The optimization is carried out for two cases. In the first case, quasi-steady aerodynamic model is employed in the rotor analysis and in the second case, unsteady aerodynamic model with both attached flow and impulsive aerodynamics is used. The unsteady aerodynamics are based on the Leishman model [22].

1)Quasi-steady Aerodynamic Model: In previous studies, quasi-steady aerodynamics has been used in the rotor dynamic analysis [1]. To see the influence of the unsteady aerodynamic model, optimization is carried out first with the quasi-steady model. A variation of 25 and 5 percent is taken from the baseline values of torsional stiffness and the mass of the blade, respectively. As per the DOE theory, 9 ($i.e, 2^2 + 2 * 2 + 1 = 9$) points are selected in the design space. The objective function values are evaluated at the selected points, using the UMARC code. A RS model is developed with these results, which is shown in the figure(2),

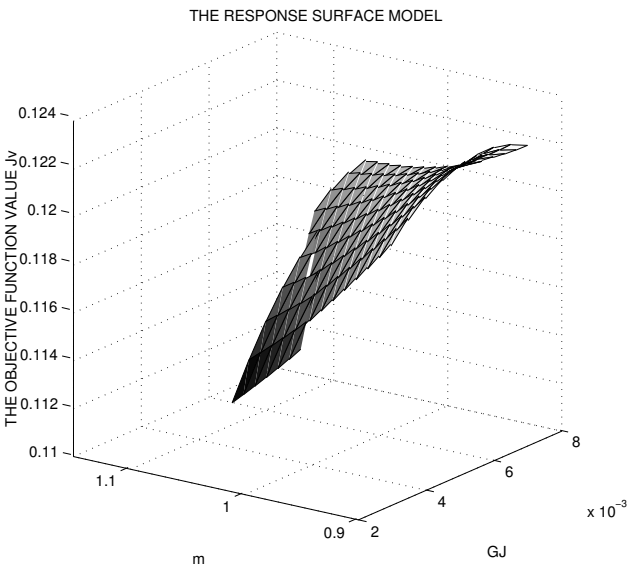

Figure 2: RS with quasisteady model about baseline design ($\triangle GJ = 25\%, \triangle m = 5\%$)
$J_v = 0.2719 - 3.9027GJ - 0.2520m - 338.4307GJ^2 + 0.08m^2 + 9.106GJ * m$

where the GJ and m represents the torsional stiffness and the blade mass, respectively. The second order response surface function is also given at the bottom of the figure.

Then optimization is carried out using gradient based method. Constraints are imposed on the function to ensure that the design variables remain in the region, where the response surface is valid. This is assured by constraining the design variables to remain in the circle as shown in the figure(1).

The results of the optimization shows a reduction of 4.08% in the objective function value J_v. And the non-dimensional optimum design values are $GJ = 0.004454, m = 1.0442$. This reduction is achieved with a decrease in the torsional stiffness and a slight increase in the mass from the baseline design value.

2) Unsteady Aerodynamic Model: In this case,

and for all future results, unsteady aerodynamic model is employed in the rotor analysis code. To search for the global minima, the optimization is carried out in different stages. The size of the design space is reduced in each stage, by which the accuracy of the RS model is increased while reaching the global minimum. The optimization process is terminated when one of the constraints become active. The stages of optimization are discussed below.

In the first stage of optimization, a variation of 25 and 5 percent is taken from the baseline values of torsional stiffness and the mass of the blade, respectively. Then, the optimization is carried out as discussed in the quasi-steady state case. The RS model developed for this stage is shown in the figure (3).

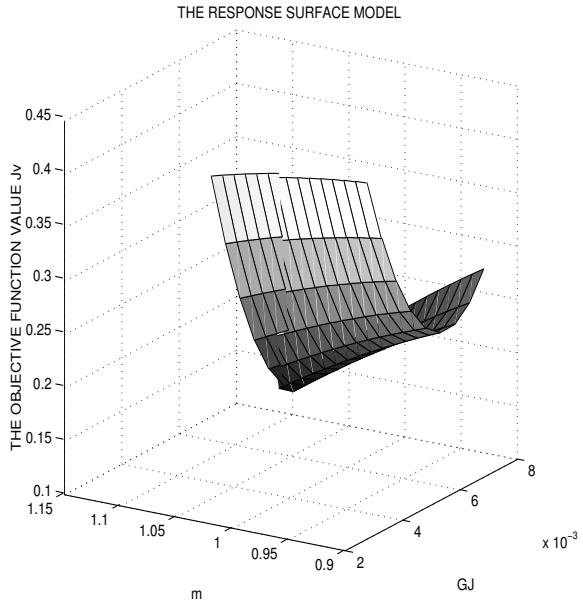

Figure 3: RS with unsteady model about baseline design ($\triangle GJ = 25\%, \triangle m = 5\%$)
$J_v = 0.0232 - 177.95GJ + 2.208m + 24113.19GJ^2 - 0.88m^2 - 156.1GJ * m$

In this stage, the J_v is reduced by 7.15 percent from its initial value, for the values of design variables, $GJ = 0.007$ and $m = 1.065$. The results obtained in this case show that value of mass has to be increased and torsion stiffness also increased slightly from the initial baseline design value for reduction in the objective function value. Also, the RS model developed for the above two cases (shown in fig(2) & fig(3)) are different, with in the same design space. This is found to be because of the strong influence of torsional stiffness, on the unsteady impulsive pitching moments. This clearly shows the significance of the unsteady aerodynamic model in the optimization process. The adequacy of the model developed is checked. The residuals versus fitted values is plotted for the model developed, as given in figure(4). The plot does not reveal any obvious pattern and therefore the response surface chosen is adequate.

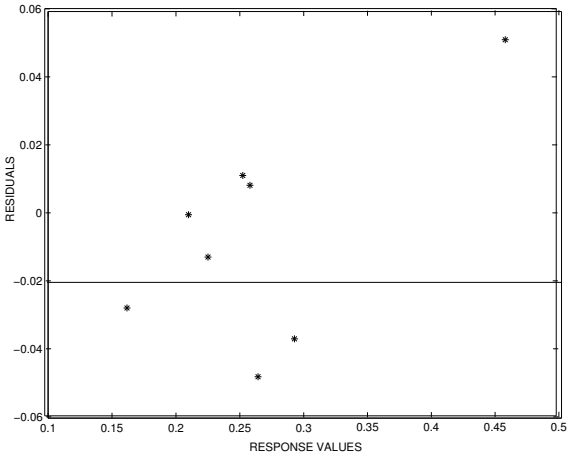

Figure 4: Plot of residuals versus fitted values for model,
$J_v = 0.0232 - 177.95GJ + 2.208m + 24113.19GJ^2 - 0.88m^2 - 156.1GJ * m$

The optimum values of the first stage are taken as the initial design values for the next stage. The perturbations in m and GJ are made progressively smaller as the iteration progress. At the second stage, the design space is created with a variation of 15 and 3 percent along the torsional stiffness and the mass, respectively. In each stage, the constraints (20) and (7) are checked and the optimization is proceeded. In the third stage, a variation of 5 and 1 percent are taken in the torsional stiffness and mass respectively. The RS model developed for the second stage is shown in the figure(5). The residuals versus the fitted values for the model in figure(5) is shown in figure(6). The RS model developed for the third stage is shown in the figure(7). The residuals versus the fitted values for the model in figure(7) is shown in figure(8). In both the figures (6) and (8) the plot does not reveal any obvious pattern. So the response surface models developed are considered to be adequate.

A reduction of 5.28 and 3.31 percent is achieved in the second and third stage, respectively. At the third stage, the constraint J_{d1} becomes active and the optimization process is terminated. Finally, a total reduction of 15.74 percent is achieved, for the objective function J_v. This is accomplished through three stages of optimization where response surfaces are created and optimization is carried out at each stage.

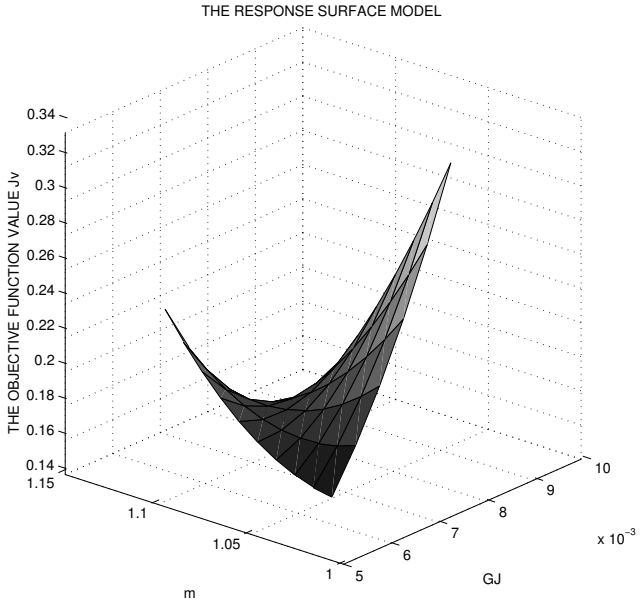

Figure 5: RS model for second stage ($\triangle GJ = 15\%, \triangle m = 5\%$)
$J_v = 2.1877 + 1126.89GJ - 10.433m + 8939.8GJ^2 + 8.3184m^2 - 1159.37GJ * m$

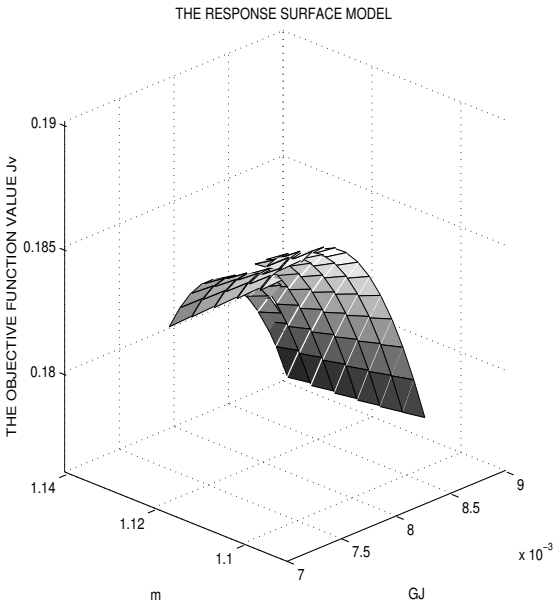

Figure 7: RS model for third stage ($\triangle GJ = 5\%, \triangle m = 1\%$)
$J_v = 0.7314 + 19.4041GJ - 0.9939m - 9632.49GJ^2 + 114.4797GJ * m$

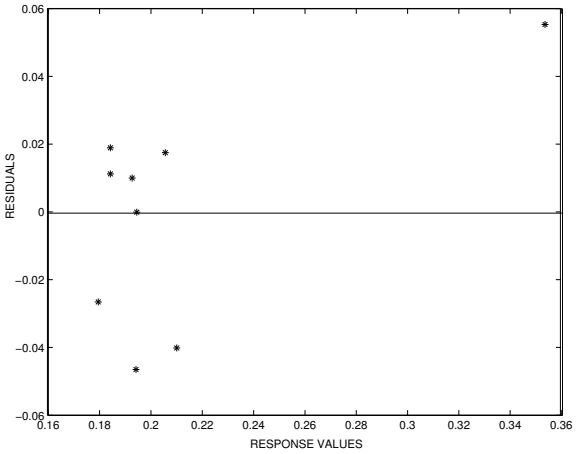

Figure 6: Plot of residuals versus fitted values for model,
$J_v = 2.1877 + 1126.89GJ - 10.433m + 8939.8GJ^2 + 8.3184m^2 - 1159.37GJ * m$

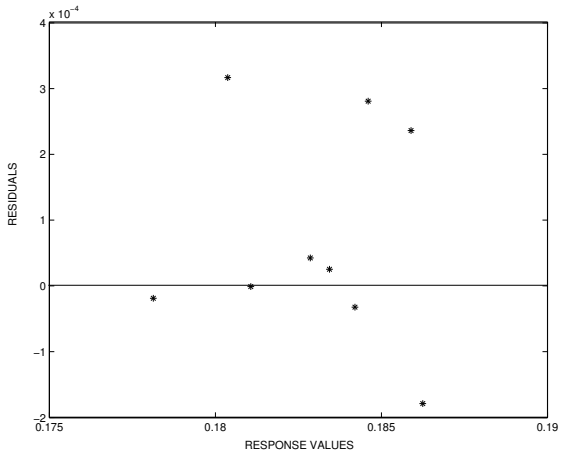

Figure 8: Plot of residuals versus fitted values for model,
$J_v = 0.7314 + 19.4041GJ - 0.9939m - 9632.49GJ^2 + 114.4797GJ * m$

Since the RS models created are simple polynomials, optimization process finds the global constrained minimum point very rapidly. The interactive nature of the design process allows the termination of the optimization process at any stage with a feasible optimal design. The approach is therefore well suited for an industry setting.

Four Design Variables

In this stage, two more design variables, the flap stiffness and the lag stiffness of the rotor blades are added in the optimization process. The flap stiffness and lag stiffness of the blade are kept constant for the full span of the blade. Thus the four design variables are blade mass, flap, lag and torsional stiffness. A variation of 25 percent is taken for each of these stiffness variables and 5 percent along the mass design variable. For the four design variables, the axial distance in CCD is taken as $\sqrt{4}$. And the function is evaluated at $25(2^4 + 2*4 + 1)$ design points. With these function values, RS model created is given below .

$$\begin{aligned} J_v \quad = \quad & 52.58 - 2702.86EI_y + 1626.38EI_z \\ & -5033.19GJ - 77.4m + 11261.98EI_y^2 \\ & +5586.71EI_z^2 + 22333.57GJ^2 \\ & +28.84m^2 - 20795.47EI_y * EI_Z \\ & +2578.52m * EI_y + 47358.21GJ * EI_y \\ & +4360.02GJ * m - 1514.59EI_z * m \\ & -9800.8EI_z * GJ \end{aligned} \tag{14}$$

The RS function with the constraints (4)&(5) is then minimized. A reduction of 14.85 percent in the optimum function value is achieved in the first stage with the dynamic constraint J_{d1} becomes active.

The results from the optimization, using four design variables are presented in Table(II). At the optimum, the frequencies are reduced as shown in the Table(III).

Table II: Optimum Values

	Reference	At Optimum
EI_y	.0108	.0062
EI_Z	.0268	.0134
GJ	.00615	.0033
m	1.0	1.0999

The vibration reduction is achieved by destiffening of the blade in flap, lag and torsion directions and a small increase in blade mass. The frequencies of the lag, flap and torsion mode are reduced from the baseline values.

Table III: Blade Frequencies(per rev)

Mode	Reference*	At Optimum
lag bending	.744 (1)	.579 (1)
flap bending	1.146 (2)	1.105(2)
flap bending	3.512 (3)	3.097(3)
torsion	4.551 (5)	3.223 (4)

*the value in paranthesis is mode number

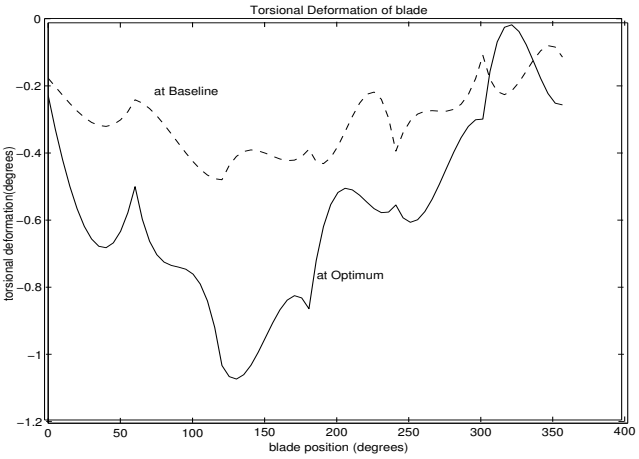

Figure 9: Tip torsional deformation variation with rotor azimuthal location

Figure(9) shows the torsional response of the blade for the baseline and optimal designs. The response is complicated due to the use of unsteady aerodynamic models including impulsive pitching moments. Figure(10) shows the 4/rev hub forces for the baseline and optimal design. Figure (11) shows the 4/rev hub moments for the baseline and optimal design. The dominant component of the 4/rev hub forces in this case is the 4/rev vertical shear and is reduced by 23 percent.

This comes at the expense of a increase of 51.8 percent and 35 percent in the longitudinal and lateral 4/rev hub forces, respectively. Figure (11) shows the 4/rev hub moments for the baseline and optimal design. The dominant component of the 4/rev hub moments are the rolling and pitching moments in this case. These are reduced by 22.5 and 26 percent, respectively. The relatively smaller yawing moment is also reduced by 49.7 percent.

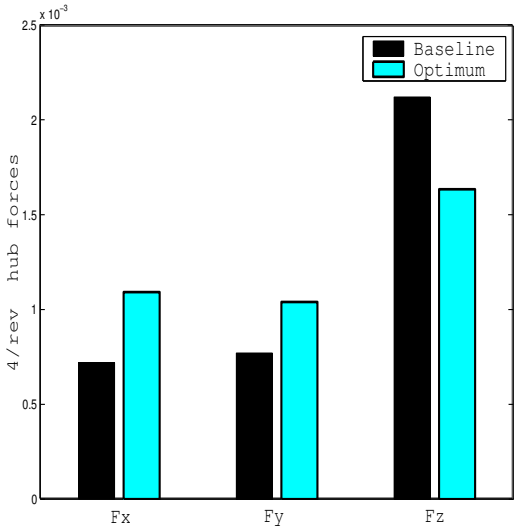

Figure 10: Vibratory forces on the rotor hub

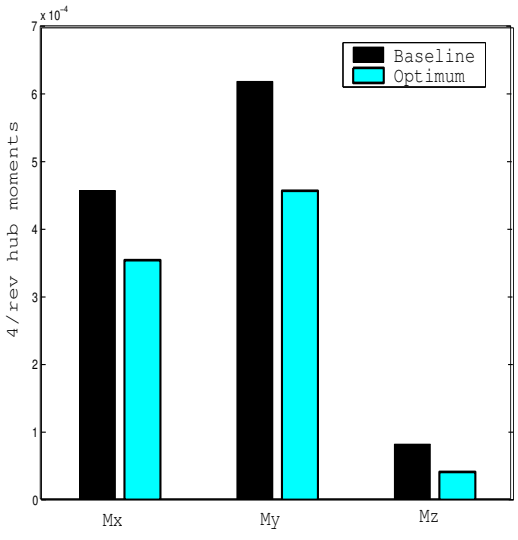

Figure 11: Vibratory moments on the rotor hub

Genetic Algorithm in Cross Section Design

The above upper level optimization problem ends with optimal stiffnesses and mass for the rotor blade. With this optimal solution, the rotor blade cross section has to be designed. This method can be called as the 'inverse method' in optimization [25].

A uniform composite box beam model is considered to be designed for the optimal solution. A box beam model developed by Smith and Chopra [26] is used as the baseline model. This design of the box beam was obtained using a manual process to obtain a reasonable elastic stiffnesses for the rotor blade. The proposed design has outer dimensions of breadth b = 4.2 inch (106.68 mm) and height h= 2.2 inch (55.88 mm). Each box-beam wall has 26 plies of thickness 0.0005 inch (.0127 mm). The ply angles were $[0_3/(\pm 15)_3/(\pm 45)_2]_s$.

The above proposed box-beam model is then optimized to have the effective stiffness values near to the optimal solution of the upper level problem. Therefore, the objective function J used here represents the sum of squares of differences between the current stiffness values and the optimal stiffness values. The objective J function is of the form

$$J = \left(\frac{EI_y^f - EI_y}{EI_y^f}\right)^2 + \left(\frac{EI_z^f - EI_z}{EI_z^f}\right)^2 + \left(\frac{GJ^f - GJ}{GJ^f}\right)^2 \tag{15}$$

where EI_y, EI_z and GJ represents the flap, lag, torsional stiffnesses respectively and the superscript f represents the final or desired values.

The box beam breadth b, height h, and ply angles θ are taken as the design variables with the thickness of the box-beam walls kept constant. The box-beam design variables are then,

$$\mathbf{D} = [b, h, \theta] \tag{16}$$

The ply angle design variables can be written in a general form by extending the Smith and Chopra laminate as,

$$\theta = [\theta_1, (\pm\theta_2), (\pm\theta_3), (\pm\theta_4), (\pm\theta_5), (\pm\theta_6), (\pm\theta_7)] \tag{17}$$

The constraints are used to control the departure of the box-beam dimension from a baseline design and to avoid an unrealistic design. The constraints on b and h are

$$b^l \leq b \leq b^u \tag{18}$$

$$h^l \leq h \leq h^u \tag{19}$$

where the superscripts l and u refer to the lower and upper bounds. Constraints are also placed on the ply

angles.

$$\theta^l \leq \theta \leq \theta^u \tag{20}$$

Ply orientation angles of composite laminates are allowed to take values of 0^0,45^0 and 90^0. The upper and lower limits for breadth is 5 inch and 4 inch and, for height is 3 inch and 2 inch, repectively. The unidirectional Graphite/Epoxy prepreg plies (Hercules AS4/3501-6) is used for the composite box beam and its material properties are given in Table(IV). The objective function is then minimized using Genetic Algorithms [27]. The results of the optimizaion are shown in the Table(V). Also the box-beam design for the baseline stiffness values are give in Table(VI)

Table IV: Material Properties of Graphite/Epoxy

Properties	Values
E_L (GPa)	141.95
E_T (GPa)	9.79
G_{LT}(GPa)	5.99
ν_{LT}	0.42

Table V: Optimal Box-Beam Design

Variables	Optimal Design
breadth (inch)	4.21
height (inch)	2.68
θ_1	0^0
θ_2	90^0
θ_3	90^0
θ_4	90^0
θ_5	90^0
θ_6	45^0
θ_7	0^0
Stiffness	Section Values
GJ	0.0031
EI_y	0.0064
EI_z	0.0131

The section designed above have the effective stiffness values (given in Table V, VI) near to that required by the upper level problem (Table II). The mass of both box-beams designed is lesser than the value of the blade mass required to acheive reasonable frequencies given in Table III. Therefore, nonstructural mass can be added at the blade quarter chord to bring it to the level required by the aeroelastic analysis predictions. This addition of mass was also done by Smith and Chopra [26] to arrive at a feasible rotor design.

Aeroelastic Analysis Convergence

Convergence problems were encountered in the aeroelastic analysis, at a few points identified by the CCD, when using the unsteady aerodynamics model. Therefore the rotorcraft aeroelastic analysis was converged with a relaxed convergence criteria at these points. The fragility of rotor aeroelastic analysis, when sophisticated aerodynamic models are used has been noted by some researchers [23, 24]. This problem is very important for the successful application of optimization to rotor aeroelastic problems. If the rotor aeroelastic analysis fails to converge at any point, typical optimization algorithms based on gradient or non-gradient methods will have serious problems. The 'divergence' of a non-linear analysis results in the 'divergence' of the entire optimization process. However, when constructing response surface approximations, the rotor designer is able to use his or her experience in tuning convergence parameters or initial guesses for the analysis to obtain a reasonable load prediction. Therefore, the interactive development and use of response surface approximations for the rotor aeroelastic analysis allows the use of optimization methods in helicopter industry.

Table VI: Baseline Box-Beam Design

Variables	Optimal Design
breadth (inch)	4.71
height (inch)	2.62
θ_1	0^0
θ_2	45^0
θ_3	0^0
θ_4	45^0
θ_5	45^0
θ_6	90^0
θ_7	0^0
Stiffness	Section Values
GJ	0.00647
EI_y	0.0105
EI_z	0.0264

Conclusions

The problem of vibration reduction in a 4-bladed rotor is solved using a response surface approach. The objective function are the 4/rev hub loads. Constraints are imposed on blade root dynamic stresses and bounds are placed on the design variables to keep

them in the region where the response surface approximation is valid. The lower level problem of composite box-beam design is solved using genetic algorithm. The following conclusions are drawn from this study.

1. The response surface approximations for vibratory hub loads with unsteady aerodynamic model in the rotor aeroelastic analysis and the quasi-steady aerodynamic model in the aeroelastic analysis are different. The search direction for the optimum from the baseline design is also entirely different for the two cases. The importance of unsteady aerodynamic model in the aeroelastic optimization is shown by RS approximations.

2. Second order polynomial approximations based on the central composite design are effective for rotor aeroelastic analysis, provided the design variables are restricted to a region of validity. The RS model with in the hyper sphere of radius $\sqrt{k}$ in the CCD design shows good approximation, hence can be used as the maximum move limit for the design variables in the aeroelastic optimization.

3. The problems of numerical fragility of rotor aeroelastic analysis in a few design points due to lack of convergence, especially when unsteady aerodynamic model is used, are easier to handle using the response surface approach which overfits a second order function and is able to smooth out errors.

4. The response surface approach in upper level optimization problem decouples the analysis problem from the optimization problem and can help in spreading the use of optimization methods as a design tool in the helicopter industry, where one group can develop the approximations and another group can solve the optimization problems.

5. Using the blade flap, lag and torsion stiffness, and blade mass as design variables, it is found that vibration reduction of about 15 percent is obtained using just one response surface approximation. The final design is softer in flap, lag and torsion and showed a small increase in the mass. The dominant dynamic loads which are the vertical hub shear, and rolling and pitching moments show reduction of 23, 22.5 and 26 percent, respectively.

6. Rotor aeroelastic optimization typically use one-dimensional beam stiffnesses as cross section design variables. The problem of designing a box-beam corresponding to these section properties is addressed using genetic algorithm. Results show that the GA can be used to obtain ply layups with discrete design variables $[0^o, (\pm 15^o), (\pm 45^o)]$ and also to change the dimensions of the box-structure.

References

[1] Ganguli, R., and Chopra, I. (1996). Aeroelastic Optimization of Helicopter Rotor with Two Cell Composite Blades. AIAA Journal, 34(4), 835-854.

[2] Yuan, K-A., and Friedmann, P. P. (1998). Structural Optimization for Vibratory loads Reduction of Composite Helicopter Rotor Blades with Advanced Geometry Tips. Journal of the American Helicopter Society, 43(3), 246-256.

[3] Chattopadhyay, A. and Walsh, J. L. (1990). Minimum Weight Design of Rotorcraft Blades with Multiple Frequency and Stress Constraints. AIAA Journal, 28(3), 565 - 567.

[4] McCarthy, T. R. and Chattopadhyay, A. (1996). A Coupled Rotor/Wing Optimization Procedure for High Speed Tilt Rotor Aircraft. Journal of the American Helicopter Society, 41(4), 360 - 369.

[5] Lee, J., and Hajela, P. (1996). Parallel Genetic Algorithm Implementation in Multidisciplinary Rotor Blade Design. Journal of Aircraft, 33(5), 962-969.

[6] Kim, J. E., and Sarigul-Klijn, N. (2001). Elastic-Dynamic Rotor Blade Design with Multiobjective Optimization. AIAA Journal, 39(9).

[7] Soykasap, O., and Hodges, D.H. (2000). Performance Enhancement of a Composite Tilt-Rotor Using Aeroelastic Tailoring. Journal of Aircraft, 37(5), 850-858.

[8] Celi R., (2000). Optimization-Based Inverse Simulation of a Helicopter Slalom Maneuver. Journal of Guidance, Control, and Dynamics. 23(2), 289-297.

[9] Spence, A. M., and Celi, R. (1994). Efficient Sensitivity Analysis for Rotary-Wing Aeromechanical Problems. AIAA Journal, 32(12), 2337-2344.

[10] Celi, R. (1999). Recent Applications of Design Optimization to Rotorcraft-A Survey. Journal of Aircraft, 36(1), 176-189.

[11] Lu, Y., and Murthy, V. R. (1992). Sensitivity Analysis of Discrete Periodic Systems with Applications to Helicopter Rotor Dynamics. AIAA Journal, 30(8), 1962-1969.

[12] Lim, J. W., and Chopra, I.(1991). Aeroelastic Optimization of a Helicopter Rotor Using an Efficient Sensitivity Analysis. Journal of Aircraft, 28(1), 29-37.

[13] Patrick, N.K. (1999). Statistical Approximations for Multidisciplinary Design Optimization: The Problem of Size. Journal of Aircraft, 36(1), 275-286.

[14] Venter, G., Haftka, R. T., and Starnes Jr, J. H. (1998). Construction of Response Surface Approximations for Design Optimization. AIAA Journal, 36(12), 2242-2249.

[15] Hosder, S., Watson, L. T., Grossman, B., Mason, W. H., Kim, H., Haftka, R. T., Con, S. E.(2001). Polynomial Response Surface Approximations for the Multidisciplinary Design Optimization of a High Speed Civil Transport. Optimization and Engineering, 2(4), 431-452.

[16] Henderson, J. L., Walsh, J. L., and Young, K. C. (1995). Application of Response Surface Techniques to Helicopter Rotor Blade Optimization Procedure. Proceedings of the AHS National Technical Specialist Meeting on Rotorcraft Structures: Design challenges and Innovative Solutions (Williamsburg, VA).

[17] Ganguli, R., and Chopra, I.(1996). Aeroelastic Optimization of Helicopter Rotor to Reduce Vibration and Dynamic Stresses. Journal of Aircraft, 12(4), 808-815.

[18] Hodges, D. H. and Dowell, E. H. (1974). Nonlinear Equations of Motion for the Elastic Bending and Torsion of Twisted Nonuniform Blades. NASA TND-7818.

[19] Borri, M. (1986). Helicopter Rotor Dynamics by Finite Element Time Approximations. Computer and Mathematics with Applications, 12A(1), 149-160.

[20] Bir, G., *et al.* (1992). University of Maryland Advanced Rotorcraft Code(UMARC) Theory Manual, UM-AERO Report 92-02.

[21] Myers, R. H., and Montgomery, D. C. (1995). Response Surface Methodology: Process and Product Optimization using Designed Experiments, Wiley, NewYork.

[22] Leishman, J. G., and Beddoes, T. S.(1989). A Semi-Empirical Model for Dynamic Stall. Journal of the American Helicopter Society, 34(3), 3-17.

[23] Tarzanin, F., and Young, D. K. Boeing Rotorcraft Experience with Rotor Design and Optimization. AIAA-98-4733.

[24] Tarzanin, F., Young, D. K., and Panda, B. (1999). Advanced Aeroelastic Optimization Applied to an Improved Performance, Low Vibration Rotor. Proceedings of the 55th American Helicopter Society Annual Forum, Montreal, Canada.

[25] Soykasap O. (2001). Inverse method in tilt-rotor optimization. Aerospace and Science Technology, 5, 437-444.

[26] Smith, EC., and Chopra, I. (1991). Formulation and Evaluation of an Analytical Model for Composite Box-Beams. Journal of American Helicopter Society, 36(3), 23-35.

[27] Goldberg D. Genetic Algorithms in Search, Optimization, and Machine Learning. Pearson Education Inc. 2001.